Supplementary Information

Reversible Coordination-Induced Spin State Switching in a Nickel(II) Complex *via* a Crystal-to-Crystal Transformation

Yaqian Zhao, Liang Wang, Shufang Xue* and Yunnan Guo*

Experimental section

General information. All chemicals used throughout the experiments were commercially available with analytical grade and used as received without any further purification, where all manipulations were also performed under an aerobic environment.

Synthesis of ligand H_4hbth. The ligand *N*'1,*N*'4-bis((*E*)-2-hydroxybenzylidene)terephthalohydrazide, **H_4hbth,** was prepared using literature procedures.[1]

Synthesis of complex 1·py·MeOH. To a solution of $Ni(ClO_4)_2·6H_2O$ (73.7 mg, 0.2 mmol) in methanol (10 mL) was added 20 mL methanol solution of **H_4hbth** (40.2 mg, 0.1 mmol) followed by dropwise addition of 2 mL pyridine and NaOH (8.0 mg, 0.2 mmol). The ensuing orange solution was stirred for 1 h and subsequently filtered. The filtrate was left undisturbed to allow the slow evaporation of the solvent. Orange crystals suitable for the single crystal X-ray diffraction were obtained within a few weeks. Yield, 49.8 mg (47% based on the metal salt). Anal. Calcd. (Found) for **1·py·MeOH** ($C_{54}H_{52}N_{10}Ni_2O_6$): C, 61.51 (60.89); H, 4.97 (4.92); N, 13.28 (13.14). IR (KBr, cm^{-1}): 3436(br), 3059(w), 1603(s), 1539(m), 1516(s), 1484(w), 1466(w), 1440(m), 1394(w), 1362(w), 1339(w), 1217(w), 1184(w), 1153(w), 1073(w), 1036(w), 1007(w), 883(w), 754(w), 723(w), 705(m), 667(w), 618(w), 547(w).

Synthesis of complex 1. For single-crystal X-ray diffraction measurements, a single crystal of **1** can be obtained by heating a single crystal of **1·py·MeOH** in the diffractometer under a dry N_2 flow from 300 to 400 K at a heating rate of 3 K min^{-1} and further annealing at 400 K for 30 mins. Interestingly, single crystals of **1** can be also obtained by slow diffusion in methanol using a single-tube glass vessel. A solution of the H_4**hbth** ligand (0.1 mg, 0.05 mmol), NaOH (4.0 mg, 0.1 mmol) and pyridine (3

drops) in methanol (10 mL) was placed at the top of an $Ni(ClO_4)_2 \cdot 6H_2O$ (36.9 mg, 0.1 mmol)-containing methanol solution (5 mL) for two weeks, affording red block crystals, suitable for X-ray diffraction analysis. For other measurement, the well ground crystals of **1·py·MeOH** were heated at 400 K in the dynamic vacuum for 2 h. Anal. Calcd. (Found) for **1** ($C_{32}H_{24}N_6Ni_2O_4$): C, 57.03 (56.46); H, 3.59 (3.91); N, 12.47 (12.35). IR (KBr, cm^{-1}): 3438(br), 3079(w), 1655(s), 1603(s), 1533(s), 1508(m), 1485(w), 1456(m), 1399(w), 1374(w), 1334(m), 1303(w), 1226(w), 1206(m), 1151(w), 1104(w), 1072(w), 1045(w), 945(w), 905(w), 801(w), 834(w), 755(m), 744(m), 734(w), 709(m), 689(m), 663(m), 615(w), 535(w), 506(w).

Synthesis of 1·py·MeOH-re. The samples of **1** were exposed at room temperature to a mixture of pyridine and methonal (20:80, V:V) atmosphere for one day.

Vapor diffusion of volatile organic compounds. The small amount of fresh crystals of **1** (ca. 120 mg) was added to a small glass vial and the vial was placed in a larger-capped glass vial with corresponding solvent inserted (ca. 1 mL). The whole assembly was sealed and allowed to stand until crystals turns to colors thanks to vapor diffusion. Then the setup was launched to the Gouy balance for monitoring the magnetic susceptibility change based on CISSS. Meanwhile, the color-changed sample was collected, then ground for the DRS and PXRD measurement. All the samples can be saturated under different vapor with sufficient time, without the observation of dissolving by the overload of vapor diffusion.

Characterization techniques

Elemental analysis for carbon, hydrogen, and nitrogen were carried out on a Perkin-Elmer 2400 analyzer. Infrared spectra (IR) were recorded on a Nicolet iS10 FT-IR instrument with KBr pellets. Thermogravimetric analysis (TGA) were performed in $N_{2(g)}$ (100 mL min^{-1}) at a heating rate of 2 and 10 K min^{-1} from 298 to 873 K using a Mettler Toledo TGA/SDTA 851e analyzer. Powder X-ray Diffraction (PXRD) experiments were carried out on a D8 Advanced diffractometer from Bruker. The diffractogram was recorded using CuKα radiation (λ = 1.5406 Å) and a linkeye XE-T detector (Bruker) in the 5-50° (2θ) range with an increment of 0.00151° and an integration time of 0.15 s. Diffuse-reflectance UV-Vis-spectra (DRS) were recorded using a Shimadzu Perkin Elmer Lambda 9 UV-vis spectrophotometer. $BaSO_4$ powder was used as the reference (100% reflectance). UV-vis spectroscopic measurements were performed with a UT6A UV-vis spectrophotometer. The titration

experiments of complex **1** at fixed concentration of 10^{-5} mol L^{-1} were taken in toluene, pyridine and mixtures of the two solvents. All photographs were recorded on a mobile phone under UV light (365 nm). Magnetic susceptibility measurements for both complexes were carried out on a MPMS3 SQUID magnetometer in the direct current (DC) mode, under an applied magnetic field of 1000 Oe. The magnetic data were corrected for the diamagnetic contributions. The measurement of *in situ* magnetic susceptibility (χ_M) for monitoring the CISSS was measured by Faraday method as the previous work.[2]

Crystallographic data for complex **1·py·MeOH** and **1** were collected using Mo-Kα (λ = 0.71073 Å) radiation. The crystals were selected, mounted in inert oil and transferred to the cold gas stream for flash cooling. Data were integrated by Crysalis (Agilent Technologies (2012). Agilent Technologies UK Ltd., Oxford, UK, Xcalibur/SuperNova CCD system, CrysAlisPro Software system, Version 1.171.36.21). Absorption correction was applied using the integrated multi-scan absorption algorithm. The structures were solved by direct methods (SHELXS) and refined by full-matrix least-squares on $|F^2|$ using SHELXL2014.[3] All nonhydrogen atoms were refined with anisotropic temperature factors. Aromatic H atoms were placed at calculated positions and ride on the parent atom. CCDC 2171269 (**1·py·MeOH**) and 2171268 (**1**) are the supplementary crystallographic data for this paper. They can be obtained free of charge from the Cambridge Crystallographic Data Center *via* www.ccdc.cam.ac.uk/data_request/cif.

UV-Vis titration of 1 with pyridine to evaluate the constants K_1 and K_2

Provided that that the paramagnetic complexes **1·(py)** and **1·$(py)_2$** have similar absorption maxima (λ_{max}) and extinction coefficients (ε), K_1 and K_2 can be estimated from the decrease of the band of the uncoordinated **1** at 372 nm.

The correlation between the concentration of diamagnetic species and that of added pyridine can be derived as follows[4]:

$$\frac{C_0}{C_{\text{dia}}} = 1 + K_1 C_{py} + K_1 K_2 C_{py}^2$$

C_0: initial concentration of **1**;

C_{dia}: concentration of diamagnetic species;

C_{py}: concentration of added pyridine;

K_1 and K_2: the constants corresponding to the ligation of one and two axial donors, respectively.

The measurement of *in situ* magnetic susceptibility (χ_M)

χ_M for monitoring the CISSS was measured by Faraday method, the magnetic force is defined by:

$$f_x = m\chi H_0 \frac{dH}{dX} \text{ and } \chi_M = \frac{M\chi}{\rho} \qquad (1)$$

in which, m = mass of sample; χ = volume magnetic susceptibility; H_0 = magnetic field strength at sample site; dH/dx = the field gradient along magnetic force direction.

On the other hand, the magnetic force can be obtained by the change of Gouy balance before and after magnetic field applied.

$$f_x = (\Delta W_{S+V} - \Delta W_V)g \qquad (2)$$

ΔW_{S+V} = apparent difference of **V**ial with **S**ample after and before magnetic field applied; ΔW_V = apparent difference of empty **V**ial after and before magnetic field applied; g = gravitational acceleration.

Combining equation (1) and (2) can deduct the final χ_M value for the corresponding samples. In our experiment, $FeSO_4 \cdot 7H_2O$ was used for a calibration, whose $\chi_M = 1.02*10^{-2}$ cm^3/mol at RT; $\rho = 1.895$ g/cm^3. The density data of **1·py·MeOH** and **1** are obtained from crystallographic calculations as shown in CIF.

Table S1. Selected Bond lengths (Å) and angle (º) for complexes **1·py·MeOH** and **1**

Complex **1·py·MeOH**		Complex **1**	
Ni1-N1	1.9878(16)	Ni1-N1	1.8347(18)
Ni1-N3	2.0676(17)	Ni1-N3	1.9518(18)
Ni1-N4	2.2196(17)	Ni1-O1	1.8214(15)
Ni1-N5	2.1747(17)	Ni1-O2	1.8498(15)
Ni1-O1	1.9939(13)	N1-Ni1-O1	94.92(8)
Ni1-O2	2.0330(13)	N1-Ni1-O2	83.45(8)
N4-Ni1-N1	88.27(6)	N3-Ni1-O1	89.76(7)
N4-Ni1-N3	88.53(6)	N3-Ni1-O2	91.86(7)
N4-Ni1-O1	93.05(6)	O1-Ni1-O2	178.72(7)
N4-Ni1-O2	85.83(6)	N1-Ni1-N3	175.29(8)
N5-Ni1-N1	88.99(6)		
N5-Ni1-N3	93.89(7)		
N5-Ni1-O1	91.57(6)		
N5-Ni1-O2	89.20(6)		
N1-Ni1-O1	92.03(6)		
N1-Ni1-O2	79.04(6)		
O1-Ni1-O2	171.03(5)		
N3-Ni1-O1	92.00(6)		
N3-Ni1-O2	96.86(6)		
N3-Ni1-N1	174.97(7)		
N4-Ni1-N5	174.70(6)		

Table S2 Intermolecular hydrogen bonding for **1·py·MeOH** and **1**

Complex	Supramolecular interaction	D-H···A	H···A/ Å	D···A/ Å	D-H···A/°	Symmetry code
1·py·MeOH	Inter-H-bond	O3-H3···N2	2.01	2.811(3)	166	-1+*x*, *y*, *z*
		C4-H4···O2	2.59	3.487(2)	163	1/2+*x*, 1/2-*y*, -1/2+*z*
		C23-H23···N2	2.48	3.412(3)	177	3/2-*x,* 1/2+*y,* 3/2-*z*
1	Intra-H-bond	C14-H14···N2	2.45	3.350(3)	157	-1/2+*x*, 1/2-*y*, 1/2+*z*

Table S3 Analysis of *Cg*···*Cg* Interactions for **1**

*Cg*I···*Cg*J[a]	Symmetry code	*Cg*···*Cg*[b] / Å	CgI_Perp[c] / Å	*Cg*J_Perp[d] / Å
*Cg*1···*Cg*3	-*x*, 1-*y*, 1- *z*	3.6266(12)	3.3683(8)	3.2988(9)
*Cg*2···*Cg*3	-*x*, 1-*y*, 1- *z*	3.3652(12)	3.2063(8)	3.2849(9)
*Cg*3···*Cg*1	-*x*, 1-*y*, 1- *z*	3.6266(12)	3.2988(9)	3.3683(8)
*Cg*3···*Cg*2	-*x*, 1-*y*, 1- *z*	3.3652(12)	3.2849(9)	3.2063(8)

[a]*Cg*1 is the centroid of five-membered ring containing Ni1, O2, O8, N2 and N1 atoms; *Cg*2 is the centroid of six-membered ring containing Ni1, O1, C2, C1, C7 and N1 atoms; *Cg*3 is the centroid of six-membered ring containing N3, C12, C13, C14, C15 and C16 atoms. [b] Distance between ring centroids. [c] Perpendicular distance of Cg(I) on ring J. [d] Perpendicular distance of *Cg*(J) on ring I.

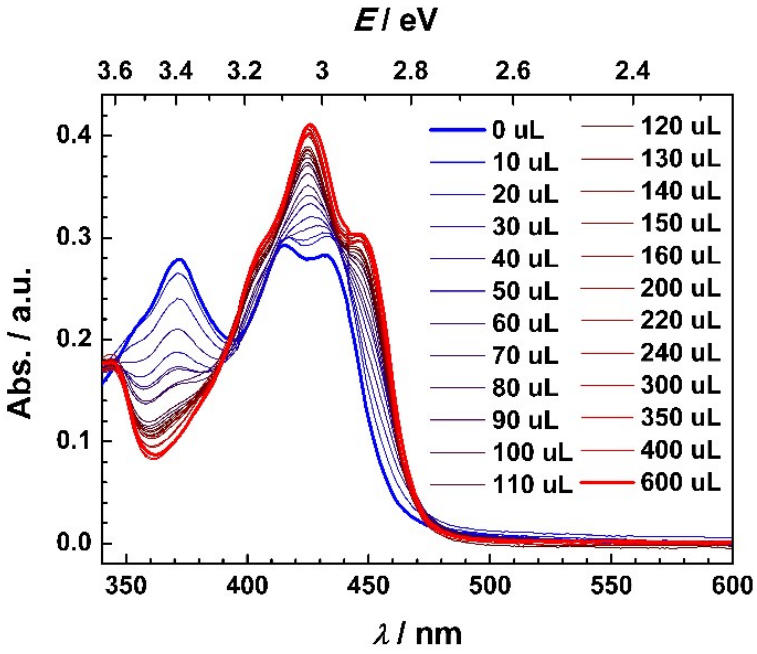

Fig. S1 Absorbance measurements of **1** in varying the volume of toluene/pyridine ratios at room temperature; the concentration of **1** is fixed at 10^{-5} mol L^{-1}. The volume of added pyridine is shown in the legend.

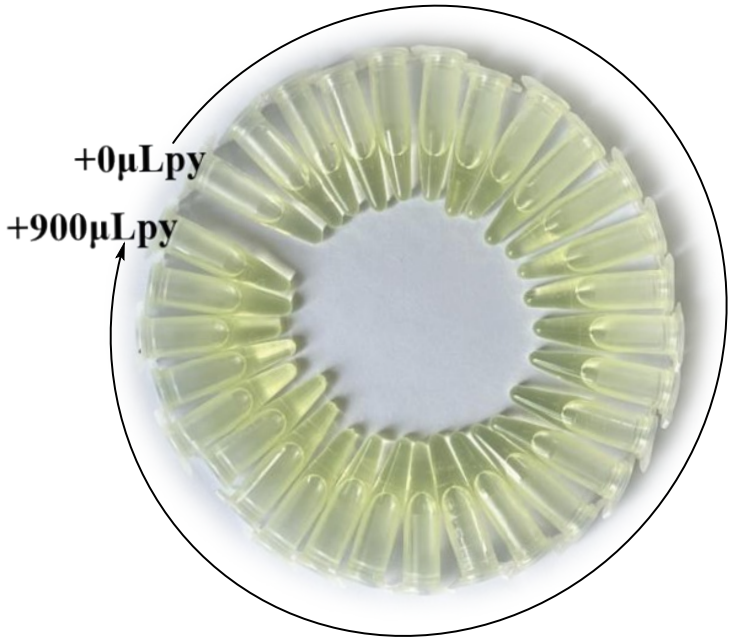

Fig. S2 Photographs of **1** in toluene/pyridine solutions.

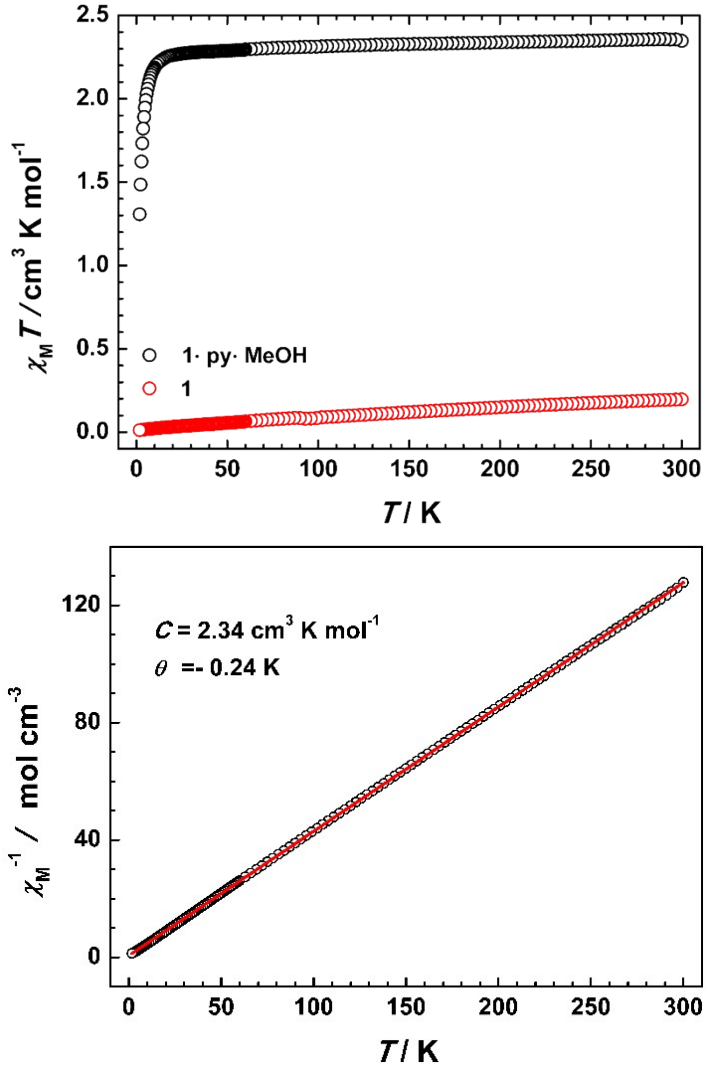

Fig. S3 (top) $\chi_M T$ versus T curves for **1·py·MeOH** and **1**; (bottom) χ^{-1} *versus* temperature plot for **1·py·MeOH** obeying the Curie-Weiss law.

Reference:

1. X. Ma, S. Liu, Z. Zhang, Y. Niu and J. Wu, A novel thermo-responsive supramolecular organogel based on dual acylhydrazone: fluorescent detection for Al^{3+} ions. *Soft Matter*, 2017, **13**, 8882.
2. S. Xue, G. F. B. Solre, X. Wang, L. Wang and Y. Guo, Vapor-triggered reversible crystal transformation of a nickel-based magnetic molecular switch. *Chem. Commun.*, 2022, **58**, 1954.
3. G. Sheldrick, A short history of SHELX. *Acta Crystallogr., Sect. A*, 2008, **64**, 112.
4. S. Thies, C. Bornholdt, F. Köhler, F. D. Sönnichsen, C. Näther, F. Tuczek and R. Herges, Coordination-Induced Spin Crossover (CISCO) through Axial Bonding of Substituted Pyridines to Nickel–Porphyrins: σ-Donor versus π-Acceptor Effects. *Chem. - Eur. J.*, 2010, **16**, 10074.